Published in final edited form as:
Trends Neurosci. 2013 March ; 36(3): 185–194. doi:10.1016/j.tins.2012.10.001.

Sustaining rapid vesicular release at active zones: potential roles for vesicle tethering

Stefan Hallermann[1] and **R. Angus Silver**[2]

[1]European Neuroscience Institute Göttingen, Grisebachstrasse 5, 37077 Göttingen, Germany

[2]Department of Neuroscience, Physiology and Pharmacology, University College London, Gower Street, London WC1E 6BT, UK

Abstract

Rapid information processing in our nervous system relies on high-frequency fusion of transmitter-filled vesicles at chemical synapses. Some sensory synapses possess prominent electron-dense ribbon structures that provide a scaffold for tethering synaptic vesicles at the active zone (AZ), enabling sustained vesicular release. Here, we review functional data indicating that some central and neuromuscular synapses can also sustain vesicle-fusion rates that are comparable to those of ribbon-type sensory synapses. Comparison of the ultrastructure across these different types of synapses, together with recent work showing that cytomatrix proteins can tether vesicles and speed vesicle reloading, suggests that filamentous structures may play a key role in vesicle supply. We discuss potential mechanisms by which vesicle tethering could contribute to sustained high rates of vesicle fusion across ribbon-type, central, and neuromuscular synapses.

Introduction

Rapid inter-neuronal communication is typically mediated by the release of neurotransmitter at cell–cell contacts termed chemical synapses, where neurotransmitter-filled vesicles fuse with the plasma membrane at specialized sites termed AZs [1]. At some sensory synapses, large electron-dense ribbon-like structures, which accumulate synaptic vesicles at the AZ, help to convert analog signals from sensory receptors into phasic and sustained vesicular release (reviewed in [2]). The fidelity and speed of the sensory representation depends on fast and repetitive vesicular release at these specialized early-stage synapses [3–5]. Many types of sensory signals are then converted into an action-potential-based rate code before being rapidly transmitted to the central nervous system for processing. Firing rates of neurons in the sensory pathways can reach frequencies as high as 1 kHz [6,7], and rates of hundreds of hertz can be sustained for long periods [8]. To transmit these high-frequency inputs, some central synapses sustain high rates of vesicle fusion [9–13], comparable to the rates found at sensory ribbon-type synapses (see below and Table 1) [4,14,15]). Firing rates of neurons in the motor pathways can also reach high levels (~100 Hz), and firing rates ~20 Hz can be sustained for minutes [16]. This raises the question of how these central synapses and neuromuscular junctions (NMJs), which lack specialized ribbon structures that accumulate vesicles at the AZ, can transmit broad-bandwidth rate-coded sensory and motor command information effectively over sustained periods of time.

Europe PMC Funders Author Manuscripts

Small electron-dense structures that are reminiscent of ribbons have been found at central and NMJ synapses (reviewed in [17]), but recent technical advances in electron microscopy suggest that their appearance may depend on the fixation procedure (reviewed in [18]). Electron-dense structures following chemical fixation appear as a network of fine vesicle-tethering filaments when rapid freeze and stain-free approaches are used together with electron tomography (reviewed in [19,20]), although some filaments that link vesicles to the ribbon and to the plasma membrane can be resolved with chemical fixation (e.g., [21,22]). Electron-dense structures at the NMJ have been shown to consist of a scaffold of distinct filaments that can tether vesicles when high-pressure freezing [23,24] and high-resolution tomography was used [25]. These data support the idea that fine filamentous structures of various lengths are common to AZs at ribbon-type, central, and NMJ synapses. Moreover, recent studies at these three types of synapses indicate that the number of tethered vesicles decreases during synaptic activity [25,26], and that interference with vesicle tethering or putative vesicle-tethering proteins [22,27–29] impairs sustained vesicular release. Here, we review the mechanisms underlying vesicle reloading during sustained activity and discuss the potential roles that vesicle tethering could play in fast and sustained vesicular release across ribbon, central, and NMJ synapses.

What are the processes involved in vesicle reloading?

According to the conventional view, to become release-competent, a transmitter-filled vesicle must first move to and then attach (dock) to the AZ plasma membrane. The docked vesicle is then converted into a state of release-competence by proteins such as SNAREs (soluble NSF attachment protein receptors), SM (Sec1/Munc18-like) proteins, and low-affinity Ca^{2+} sensors that trigger fast vesicle fusion (reviewed in [18,30]). In addition to this ‘molecular priming’, vesicles must colocalize with Ca^{2+} channels, which provide the high Ca^{2+} concentrations required to trigger fusion rapidly (‘positional priming’; reviewed in [31,32]). During sustained activity, once all the docked and primed vesicles (i.e., the release-ready pool: RRP; Box 1) are released, release may be limited by the translocation of new vesicles to the docking site(s) within the AZ, their molecular and positional priming, and/or the clearance of membrane and protein debris of fused vesicles [33–35]. For the latter, the speed of endocytosis might be important [36,37]. Thus, during sustained transmission, repetitive fusion of synaptic vesicles at a release site involves a complex sequence of events, which we refer to as ‘vesicle reloading’.

Measuring the speed of vesicle reloading

Various techniques have been developed to measure vesicular release directly. These include optical reporters, amperometric techniques, and presynaptic capacitance measurements, which have specific advantages and disadvantages in terms of temporal resolution, sensitivity, invasiveness, and applicability (e.g., [38–40]). A common, but less direct, approach used to measure vesicle reloading under intact conditions has been to measure the postsynaptic current that often decreases during sustained activity, reflecting activity-dependent synaptic depression. Depression can be caused by both pre- and postsynaptic mechanisms, with vesicle depletion and receptor desensitization (e.g., [41]), respectively, being the most common. However, other presynaptic mechanisms such as

Ca^{2+}-dependent modulation of the presynaptic Ca^{2+} currents [42–45], or inhibition by presynaptic autoreceptors [46], can be the dominating cause for depression, in particular at lower transmission frequencies or during post-tetanic depression. Even when only vesicle depletion is considered, the time-course and extent of activity-dependent depression, reflect a complex interplay between the size of the RRP, the release probability per release-ready vesicle (p_{rv}), and the rate of vesicle reloading (k).

By contrast, the recovery from synaptic depression is more directly related to the rate of vesicle reloading because it is independent of the size of the RRP (Box 1). Under these conditions only the time-dependences of p_{rv} (e.g., due to various mechanisms of facilitation) and k need to be disentangled to determine the reloading rate-constant. To do this, k can be estimated from the onset of, and recovery from, depression by applying quantal modeling of release that includes short-term facilitation [9,29,47,48]. Interestingly, a temperature increase from room to physiological temperatures doubles k without effecting RRP or p_{rv} [29,49], consistent with the idea that the kinetics of vesicle reloading is rate limiting.

Activity-dependent speeding of vesicle reloading

The kinetics of recovery of release have been analyzed at ribbon-type, NMJ, and central synapses (but here we restrict our review of the latter to excitatory cerebellar and auditory synapses because they are specialized for sustained signaling; see also [38,39]). Two components of recovery have been observed at all three types of synapse (Figure 1; see τ_{fast} and τ_{slow} in Table 1). The rapid component of recovery often becomes more apparent with stronger synaptic activity (e.g., [29,50–52]). Indeed, the amount of synaptic depression observed during activity is less than one would expect, based on the slower recovery from depression [53]. These observations suggest that the rate of vesicle reloading increases during activity at some synapses (reviewed in [32,54–56]). However, activity-dependent changes in the time-course of recovery of release could also be affected if the size of the RRP changes with activity, or if p_{rv} changes with activity due to facilitation. Interestingly, the fast component of recovery of release was altered at a ribbon synapse (Figure 1a), a central synapse (Figure 1b), and the *Drosophila* NMJ (Figure 1c), when putative vesicle tethering cytomatrix proteins (Box 2) were deleted. These data suggest that vesicle tethering plays a role in vesicle reloading and in particular in the activity-depended speeding of vesicle reloading.

Comparing the speed of vesicle reloading at different synapses

To aid cross-synapse comparison, we express the rate of vesicle reloading per release-ready vesicle, thereby taking account of the size of the RRP [57,58], or by assuming k was the reciprocal of the recovery time-constant in the absence of a more direct estimate (Box 1). The estimated rates of vesicle reloading per release-ready vesicle differ by more than one order of magnitude, even for structurally and functionally similar synapses (Table 1, Box 3). Likely reasons for these discrepancies include the difficulties in determining the size of the RRP (Box 1) and simplifying assumptions used in estimating k in some studies. Presynaptic voltage-clamp recordings tend to reveal a larger RRP, and therefore possibly give a lower estimate of the vesicle reloading rate-constant, because they allow the application of

stronger stimuli compared with extracellular axonal stimulation. Moreover, vesicle fusion can be determined with presynaptic capacitance measurements independently of possible contamination by postsynaptic receptor saturation or desensitization [32]. However, it is unclear how the rates obtained with strong biophysical stimuli (e.g., prolonged presynaptic voltage depolarization) relate to those that occur during brief action potentials. Indeed, strong biophysical stimuli might release remote vesicles that cannot be released with action potentials, by increasing the spatial and temporal extent of the intracellular Ca^{2+} concentration [31,59]. Thus, some of the dispersion in the estimated rate of vesicle reloading is likely to arise from methodological differences. Nevertheless, the considerable overlap in the spread of reloading rate-constants at ribbon-type, central, and NMJ synapses, is consistent with the idea that similar mechanisms are involved in sustaining transmission at different types of synapses [14]. However, the rate of vesicle reloading per AZ is higher in ribbon compared to non-ribbon-type synapses, due to the high number of release-ready vesicles per AZ at ribbon synapses (reviewed in [60]). For example, capacitance measurements revealed 12–15 release-ready vesicles per ribbon of bullfrog amphibian papilla hair cells, consistent with the number of docked vesicles in complete ultrastructural reconstructions [61].

Does efficient vesicle reloading require vesicle tethering?

Vesicle reloading involves a complex sequence of steps including translocation and molecular and positional priming. The SNARE proteins [30] can be viewed as tethers that interact with the vesicle late within the docking/priming process to mediate vesicle fusion. Recent work showing that deletion of the cytomatrix proteins Bassoon and Bruchpilot slows down vesicle reloading suggests that these and other putative vesicle tethers (Box 2) are actively involved in some of the steps before vesicle fusion (Figure 1) [22,27,29]. Moreover, recent improvements in electron microscopy (reviewed in [18–20]) have revealed a range of vesicle-tethering structures at ribbon-type, central, and NMJ synapses (Figure 2). The function of vesicle tethering has been analyzed in most detail at synapses containing ribbons (reviewed in [2]), which are classically considered as vesicle-transport structures that deliver vesicles to the AZ (‘conveyer belt’) [62]. Although additional functions have been demonstrated, such as compound fusion [63], multivesicular release [64], restricting Ca^{2+} diffusion [61], clustering of Ca^{2+} channels [22,65], and even constraining vesicle delivery [66], the importance of vesicle-tethering ribbons for vesicle reloading has recently been demonstrated by acute disruption [28] or deletion of the ribbon (Figure 1a) [22].

At central synapses, impaired vesicle tethering but no detectable changes in vesicular release were observed in Bassoon–Piccolo double mutants, suggesting that tethering of vesicles was not rate-limiting under the investigated conditions [67]. However, higher-frequency sustained synaptic transmission at cerebellar mossy fiber to granule cell synapses was significantly impaired in Bassoon mutants, due to a slowed vesicle-reloading rate during synaptic activity (Figure 1b) [29]. In contrast to Bassoon, the AZ protein Rim, which may also be involved in tethering vesicles (Box 1), is essential for basal synaptic transmission [68,69].

The most direct evidence for a causal relationship between tethering and reloading has recently been obtained at the *Drosophila* NMJ. The powerful molecular and genetic approaches available in *Drosophila* allowed a specific impairment of vesicle tethering by deletion of a small domain of the cytomatrix protein Bruchpilot, resulting in impaired sustained vesicular release (Figure 1c) [27].

Finally, electron microscopy has revealed a loss of tethered vesicles during synaptic activity. At ribbon synapses, synaptic activity reduced the number of vesicles tethered at the base of the ribbon [4,66,70]. At central synapses, activity-dependent analysis of tethering suggests that long, SNARE-independent filaments initially tether the vesicles to the AZ and then give way to multiple shorter ones in a SNARE-dependent transition [26]. In a comparable study at the frog NMJ, specific filaments (spars and ribs; Figure 2c) less frequently linked vesicles to the plasma membrane, and other filaments (pins) were longer during synaptic activity compared to resting conditions [25]. In summary, a growing number of studies suggest that vesicle tethering supports vesicle reloading. Because the fast component of recovery from synaptic depression was preferentially affected by interfering with vesicle tethering (Figure 1a–c), tethering seems to be particularly important for the speeding of vesicle reloading during high-frequency transmission.

How could vesicle tethering support vesicle reloading during sustained release?

To understand how tethering might support reloading during sustained release, we will first outline the mechanisms that are thought to underlie the speeding of vesicle reloading during activity. Two distinct (but not mutually exclusive) classes of mechanisms have been proposed that could account for the activity-dependent speeding observed at many synapses (reviewed in [32,54–56]): (i) a Ca^{2+}-dependent enhancement in the rate of vesicle reloading (Figure 3a), and (ii) two pools of vesicles: vesicles with a high release probability that are reloaded slowly, and vesicles with a low release probability that are reloaded rapidly (Figure 3b).

Mechanism 1 (Figure 3a) is based on experiments which indicate that the elevated intracellular Ca^{2+} concentration occurring during synaptic activity increases the rate of vesicle reloading. This mechanism has been proposed to account for reloading at ribbon-type [71–73], central [50,74–76], and NMJ synapses [77]. Moreover, calmodulin has been implicated in this regulation of the rate of vesicle reloading [78], probably via its interaction with Munc13 [79]. This mechanism predicts an activity-dependent fast component of recovery of release (cf. Figure 1 and Table 1) due to elevated intracellular Ca^{2+} concentration, and a slow component of recovery reflecting the basal rate of reloading.

Mechanism 2 (Figure 3b) requires that the RRP is made up of vesicles with two or more release probabilities. It has been proposed that such a heterogeneous release probability could arise from differences in the Ca^{2+}-sensitivity of the vesicles (molecular priming [80]) or from differences in the coupling distance between the Ca^{2+} channels and sensors (positional priming [32,81]). In the latter scenario, tightly coupled high p_{rv} vesicles are released first and recover slowly due to a slow positional-priming step that colocalizes them

with Ca^{2+} channels [81]. The more remote, loosely coupled low p_{rv} vesicles that are released at a slower rate can be replenished more rapidly. The p_{rv} of remote, loosely coupled vesicles may be elevated during sustained release (i.e., facilitation), due to increased intracellular Ca^{2+} concentration (i.e., enlargement of the spatial and temporal extent of $[Ca^{2+}]$; Figure 3b), thereby allowing the release of vesicles remote from the Ca^{2+} entry site. Mechanism 2 has been proposed to account for activity-dependent speeding of vesicle reloading at ribbon-type [73], central [78], and NMJ synapses [77,82]. Indeed, both Ca^{2+}-dependent and Ca^{2+}-independent models could account for the activity-dependent speeding and biphasic recovery of vesicle reloading [29,53].

Although there are several other mechanisms that could also underlie activity-dependent speeding of vesicle reloading, the evidence for them is less clear than for mechanisms 1 and 2. Because vesicle tethering is particularly relevant for activity-dependent speeding of vesicle reloading (cf. Figure 1), we tentatively suggest that vesicle tethering could support the fast reloading of vesicles by three mechanisms (Figure 3c): (i) tethering provides a reservoir of vesicles at the AZ [17], allowing the rapid delivery of vesicles during activity, (ii) tethers constrain and position vesicles close to Ca^{2+} channels (positional priming [28]), and (iii) tethers support rapid vesicle fusion by molecular interaction of the tether with vesicular proteins and other priming factors (molecular priming), enabling the vesicle to become primed as it approaches the AZ membrane. This would facilitate sustained vesicular release by allowing vesicles to fuse as soon as they reach the plasma membrane, a variant of ‘crash fusion’ as proposed in [83]. Consistent with this idea, the putative tethering proteins Bassoon and Rim interact with the ‘priming’ protein Munc13 [84,85].

Although speculative, these proposals could explain how impaired vesicle tethering and deletion of putative tethering proteins [22,27,29] seem preferentially to affect the activity-dependent speeding of reloading (i.e., the fast component of recovery; Figure 1).

Although these scenarios are attractive, it is important to keep in mind that vesicle tethers could play additional or very different roles: (i) tethers could support sustained release by binding to Ca^{2+} channels, thereby inhibiting their inactivation [86], (ii) tethering vesicles could increase the chance for compound fusion [87] by enabling ‘piggyback’ fusion, (iii) because SNARE complexes are highly fusogenic it is possible that, rather than promoting fusion, tethers actually prevent the vesicle from fusing except when the Ca^{2+}-sensing trigger is present [88]. However, this hypothesis suggests that an increase in spontaneous fusion should occur when tethers are compromised. And (iv) rather than promoting or inhibiting fusion, tethers could support the clearing of the release site from fragments of fused vesicles by accelerating endocytotic processes; in other words, vesicles could be pulled ‘inward’ by the tethers. However, at ribbon synapses, recent data argue against such a scenario: during activity, the base of the cytomatrix is depleted of vesicles [66], and vesicles originating from the cytoplasm [89] replaced vesicles at the ribbon. Whatever the precise mechanisms involved, the fact that interfering with specific cytomatix proteins impairs vesicle reloading suggests that tethers accelerate what would otherwise be a rate-limiting step for exocytosis.

Concluding remarks

The repetitive fusion of vesicles at a release site includes a highly complex sequence of processes [18,30]. During sustained rapid vesicular release, speeding of vesicle reloading has been observed at several ribbon-type, central, and NMJ synapses. The comparable kinetics and activity-dependence of vesicle reloading at these three synapse types suggest that similar mechanisms could be involved in sustaining transmission. Recent work at retinal bipolar cells [28], inner hair cells [22], cerebellar mossy-fiber synapses [29], and *Drosophila* NMJs [27] suggests that efficient speeding of vesicle reloading during synaptic activity relies on vesicle tethering [62]. Moreover, technical improvements in the analysis of the ultrastructure have revealed filamentous structures that tether vesicles at the AZs of these synapses, and alterations in tethering have been resolved during activity [25,26].

We suggest that individual tethers and filamentous scaffolds at central and NMJ synapses may play roles in vesicle supply and reloading, similar to those proposed for the much larger electron-dense structures at ribbon synapses [2,17]. Although there is little direct evidence for the molecular nature of these AZ filaments (Boxes 2 and 3), recent studies suggest that large proteins such as Bassoon, Piccolo, or *Drosophila* Bruchpilot may tether vesicles directly or indirectly to the release site. The mechanisms by which vesicle tethering could accelerate vesicle reloading is unclear, but it seems likely that vesicle tethers somehow support the repetitive guiding, docking, and priming of vesicles close to Ca^{2+} channels during high-frequency synaptic transmission (Figure 3c). However, future studies are required to elucidate the precise molecular interactions that enable fast and sustained vesicle reloading during high-frequency signaling.

Acknowledgments

We would like to thank the following for helpful discussion and critically reading previous versions of the manuscript: Jonathan Ashmore, Gerard Borst, Igor Delvendahl, Josef Dudel, Jens Eilers, Tomás Fernández-Alfonso, Eckart Gundelfinger, Manfred Heckmann, Pascal Kaeser, Tobias Moser, Erwin Neher, Jason Rothman, and Annika Weyhersmüller. S.H. received funding from the Heisenberg Program of the German Research Foundation (HA 6386/1-1 and 2-1). R.A.S. holds a Wellcome Trust Principal Research Fellowship (095667) and a European Research Council (ERC) Advanced Grant.

References

1. Katz, B. The Release of Neural Transmitter Substances. Liverpool University Press; 1969.
2. Matthews G, Fuchs P. The diverse roles of ribbon synapses in sensory neurotransmission. Nat. Rev. Neurosci. 2010; 11:812–822. [PubMed: 21045860]
3. de Ruyter van Steveninck RR, Laughlin SB. The rate of information transfer at graded-potential synpases. Nature. 1996; 379:642–645.
4. Pangršič T, et al. Hearing requires otoferlin-dependent efficient replenishment of synaptic vesicles in hair cells. Nat. Neurosci. 2010; 13:869–876. [PubMed: 20562868]
5. Cho S, et al. Recovery from short-term depression and facilitation is ultrafast and Ca^{2+} dependent at auditory hair cell synapses. J. Neurosci. 2011; 31:5682–5692. [PubMed: 21490209]
6. Rancz EA, et al. High-fidelity transmission of sensory information by single cerebellar mossy fibre boutons. Nature. 2007; 450:1245–1248. [PubMed: 18097412]
7. Jörntell H, Ekerot CF. Properties of somatosensory synaptic integration in cerebellar granule cells *in vivo*. J. Neurosci. 2006; 26:11786–11797. [PubMed: 17093099]

8. van Kan PL, et al. Movement-related inputs to intermediate cerebellum of the monkey. J. Neurophysiol. 1993; 69:74–94. [PubMed: 8433135]
9. Saviane C, Silver RA. Fast vesicle reloading and a large pool sustain high bandwidth transmission at a central synapse. Nature. 2006; 439:983–987. [PubMed: 16496000]
10. Taschenberger H, von Gersdorff H. Fine-tuning an auditory synapse for speed and fidelity: developmental changes in presynaptic waveform, EPSC kinetics, and synaptic plasticity. J. Neurosci. 2000; 20:9162–9173. [PubMed: 11124994]
11. Crowley JJ, et al. Fast vesicle replenishment and rapid recovery from desensitization at a single synaptic release site. J. Neurosci. 2007; 27:5448–5460. [PubMed: 17507567]
12. Valera AM, et al. Adaptation of granule cell to Purkinje cell synapses to high-frequency transmission. J. Neurosci. 2012; 32:3267–3280. [PubMed: 22378898]
13. Bagnall MW, et al. Frequency-independent synaptic transmission supports a linear vestibular behavior. Neuron. 2008; 60:343–352. [PubMed: 18957225]
14. Matthews G. Synaptic exocytosis and endocytosis: capacitance measurements. Curr. Opin. Neurobiol. 1996; 6:358–364. [PubMed: 8794078]
15. von Gersdorff H, et al. Evidence that vesicles on the synaptic ribbon of retinal bipolar neurons can be rapidly released. Neuron. 1996; 16:1221–1227. [PubMed: 8663998]
16. Elmqvist D, Quastel DM. A quantitative study of end-plate potentials in isolated human muscle. J. Physiol. 1965; 178:505–529. [PubMed: 5827910]
17. Zhai RG, Bellen HJ. The architecture of the active zone in the presynaptic nerve terminal. Physiology (Bethesda). 2004; 19:262–270. [PubMed: 15381754]
18. Südhof TC. The presynaptic active zone. Neuron. 2012; 75:11–25. [PubMed: 22794257]
19. Fernández-Busnadiego R, et al. Insights into the molecular organization of the neuron by cryo-electron tomography. J. Electron Microsc. (Tokyo). 2011; 60(Suppl. 1):S137–S148. [PubMed: 21844585]
20. Siksou L, et al. Ultrastructural organization of presynaptic terminals. Curr. Opin. Neurobiol. 2011; 21:261–268. [PubMed: 21247753]
21. Usukura J, Yamada E. Ultrastructure of the synaptic ribbons in photoreceptor cells of *Rana catesbeiana* revealed by freeze-etching and freeze-substitution. Cell Tissue Res. 1987; 247:483–488. [PubMed: 3494517]
22. Frank T, et al. Bassoon and the synaptic ribbon organize Ca^{2+} channels and vesicles to add release sites and promote refilling. Neuron. 2010; 68:724–738. [PubMed: 21092861]
23. Fouquet W, et al. Maturation of active zone assembly by *Drosophila* Bruchpilot. J. Cell Biol. 2009; 186:129–145. [PubMed: 19596851]
24. Stigloher C, et al. The presynaptic dense projection of the *Caenorhabditis elegans* cholinergic neuromuscular junction localizes synaptic vesicles at the active zone through SYD-2/liprin and UNC-10/ RIM-dependent interactions. J. Neurosci. 2011; 31:4388–4396. [PubMed: 21430140]
25. Szule JA, et al. Regulation of synaptic vesicle docking by different classes of macromolecules in active zone material. PLoS ONE. 2012; 7:e33333. [PubMed: 22438915]
26. Fernández-Busnadiego R, et al. Quantitative analysis of the native presynaptic cytomatrix by cryoelectron tomography. J. Cell Biol. 2010; 188:145–156. [PubMed: 20065095]
27. Hallermann S, et al. Naked dense bodies provoke depression. J. Neurosci. 2010; 30:14340–14345. [PubMed: 20980589]
28. Snellman J, et al. Acute destruction of the synaptic ribbon reveals a role for the ribbon in vesicle priming. Nat. Neurosci. 2011; 14:1135–1141. [PubMed: 21785435]
29. Hallermann S, et al. Bassoon speeds vesicle reloading at a central excitatory synapse. Neuron. 2010; 18:710–723. [PubMed: 21092860]
30. Jahn R, et al. Membrane fusion. Cell. 2003; 112:519–533. [PubMed: 12600315]
31. Eggermann E, et al. Nanodomain coupling between Ca^{2+} channels and sensors of exocytosis at fast mammalian synapses. Nat. Rev. Neurosci. 2011; 13:7–21. [PubMed: 22183436]
32. Neher E, Sakaba T. Multiple roles of calcium ions in the regulation of neurotransmitter release. Neuron. 2008; 59:861–872. [PubMed: 18817727]

33. Katz B. Neural transmitter release: from quantal secretion to exocytosis and beyond. The Fenn Lecture. J. Neurocytol. 1996; 25:677–686. [PubMed: 9023717]
34. Neher E. What is rate-limiting during sustained synaptic activity: vesicle supply or the availability of release sites. Front. Synaptic Neurosci. 2010; 2:144. [PubMed: 21423530]
35. Haucke V, et al. Protein scaffolds in the coupling of synaptic exocytosis and endocytosis. Nat. Rev. Neurosci. 2011; 12:127–138. [PubMed: 21304549]
36. Renden R, von Gersdorff H. Synaptic vesicle endocytosis at a CNS nerve terminal: faster kinetics at physiological temperatures and increased endocytotic capacity during maturation. J. Neurophysiol. 2007; 98:3349–3359. [PubMed: 17942618]
37. Hosoi N, et al. Calcium dependence of exo- and endocytotic coupling at a glutamatergic synapse. Neuron. 2009; 63:216–229. [PubMed: 19640480]
38. Lisman JE, et al. The sequence of events that underlie quantal transmission at central glutamatergic synapses. Nat. Rev. Neurosci. 2007; 8:597–609. [PubMed: 17637801]
39. Ryan TA. Presynaptic imaging techniques. Curr. Opin. Neurobiol. 2001; 11:544–549. [PubMed: 11595486]
40. Neher E. A comparison between exocytic control mechanisms in adrenal chromaffin cells and a glutamatergic synapse. Pflügers Arch. 2006; 453:261–268. [PubMed: 17016737]
41. Trussell LO, et al. Desensitization of AMPA receptors upon multiquantal neurotransmitter release. Neuron. 1993; 10:1185–1196. [PubMed: 7686382]
42. Mochida S, et al. Regulation of presynaptic $Ca_V2.1$ channels by Ca^{2+} sensor proteins mediates short-term synaptic plasticity. Neuron. 2008; 57:210–216. [PubMed: 18215619]
43. Sullivan JM. A simple depletion model of the readily releasable pool of synaptic vesicles cannot account for paired-pulse depression. J. Neurophysiol. 2007; 97:948–950. [PubMed: 17079345]
44. Forsythe ID, et al. Inactivation of presynaptic calcium current contributes to synaptic depression at a fast central synapse. Neuron. 1998; 20:797–807. [PubMed: 9581770]
45. Lin KH, et al. Similar intracellular Ca^{2+} requirements for inactivation and facilitation of voltage-gated Ca^{2+} channels in a glutamatergic mammalian nerve terminal. J. Neurosci. 2012; 32:1261–1272. [PubMed: 22279211]
46. Slutsky I, et al. Use of knockout mice reveals involvement of M2-muscarinic receptors in control of the kinetics of acetylcholine release. J. Neurophysiol. 2003; 89:1954–1967. [PubMed: 12686574]
47. Hallermann S, et al. Mechanisms of short-term plasticity at neuromuscular active zones of *Drosophila*. HFSP J. 2010; 4:72–84. [PubMed: 20811513]
48. Dittman JS, et al. Interplay between facilitation, depression, and residual calcium at three presynaptic terminals. J. Neurosci. 2000; 20:1374–1385. [PubMed: 10662828]
49. Kushmerick C, et al. Physiological temperatures reduce the rate of vesicle pool depletion and short-term depression via an acceleration of vesicle recruitment. J. Neurosci. 2006; 26:1366–1377. [PubMed: 16452660]
50. Wang LY, Kaczmarek LK. High-frequency firing helps replenish the readily releasable pool of synaptic vesicles. Nature. 1998; 394:384–388. [PubMed: 9690475]
51. Singer JH, Diamond JS. Vesicle depletion and synaptic depression at a mammalian ribbon synapse. J. Neurophysiol. 2006; 95:3191–3198. [PubMed: 16452253]
52. Wang Y, Manis PB. Short-term synaptic depression and recovery at the mature mammalian endbulb of held synapse in mice. J. Neurophysiol. 2008; 100:1255–1264. [PubMed: 18632895]
53. Wu LG, Borst JG. The reduced release probability of releasable vesicles during recovery from short-term synaptic depression. Neuron. 1999; 23:821–832. [PubMed: 10482247]
54. Borst JG, Soria van Hoeve J. The calyx of held synapse: from model synapse to auditory relay. Annu. Rev. Physiol. 2012; 74:199–224. [PubMed: 22035348]
55. Fioravante D, Regehr WG. Short-term forms of presynaptic plasticity. Curr. Opin. Neurobiol. 2011; 21:269–274. [PubMed: 21353526]
56. Regehr WG. Short-term presynaptic plasticity. Cold Spring Harb. Perspect. Biol. 2012; 4:a005702. [PubMed: 22751149]

57. Rizzoli SO, Betz WJ. Synaptic vesicle pools. Nat. Rev. Neurosci. 2005; 6:57–69. [PubMed: 15611727]
58. Alabi AA, Tsien RW. Synaptic vesicle pools and dynamics. Cold Spring Harb. Perspect. Biol. 2012; 4:a013680. [PubMed: 22745285]
59. DiGregorio DA, et al. Measurement of action potential-induced presynaptic calcium domains at a cultured neuromuscular junction. J. Neurosci. 1999; 19:7846–7859. [PubMed: 10479687]
60. Fernández-Alfonso T, Ryan TA. The efficiency of the synaptic vesicle cycle at central nervous system synapses. Trends Cell Biol. 2006; 16:413–420. [PubMed: 16839766]
61. Graydon CW, et al. Sharp Ca^{2+} nanodomains beneath the ribbon promote highly synchronous multivesicular release at hair cell synapses. J. Neurosci. 2011; 31:16637–16650. [PubMed: 22090491]
62. Lenzi D, von Gersdorff H. Structure suggests function: the case for synaptic ribbons as exocytotic nanomachines. Bioessays. 2001; 23:831–840. [PubMed: 11536295]
63. Matthews G, Sterling P. Evidence that vesicles undergo compound fusion on the synaptic ribbon. J. Neurosci. 2008; 28:5403–5411. [PubMed: 18495874]
64. Singer JH, et al. Coordinated multivesicular release at a mammalian ribbon synapse. Nat. Neurosci. 2004; 7:826–833. [PubMed: 15235608]
65. Mercer AJ, et al. Lateral mobility of presynaptic L-type calcium channels at photoreceptor ribbon synapses. J. Neurosci. 2011; 31:4397–4406. [PubMed: 21430141]
66. Jackman SL, et al. Role of the synaptic ribbon in transmitting the cone light response. Nat. Neurosci. 2009; 12:303–310. [PubMed: 19219039]
67. Mukherjee K, et al. Piccolo and bassoon maintain synaptic vesicle clustering without directly participating in vesicle exocytosis. Proc. Natl. Acad. Sci. U.S.A. 2010; 107:6504–6509. [PubMed: 20332206]
68. Han Y, et al. RIM determines Ca^{2+} channel density and vesicle docking at the presynaptic active zone. Neuron. 2011; 69:304–316. [PubMed: 21262468]
69. Kaeser PS, et al. RIM proteins tether Ca^{2+} channels to presynaptic active zones via a direct PDZ-domain interaction. Cell. 2011; 144:282–295. [PubMed: 21241895]
70. Lenzi D, et al. Depolarization redistributes synaptic membrane and creates a gradient of vesicles on the synaptic body at a ribbon synapse. Neuron. 2002; 36:649–659. [PubMed: 12441054]
71. Moser T, Beutner D. Kinetics of exocytosis and endocytosis at the cochlear inner hair cell afferent synapse of the mouse. Proc. Natl. Acad. Sci. U.S.A. 2000; 97:883–888. [PubMed: 10639174]
72. Gomis A, et al. Two actions of calcium regulate the supply of releasable vesicles at the ribbon synapse of retinal bipolar cells. J. Neurosci. 1999; 19:6309–6317. [PubMed: 10414960]
73. Babai N, et al. Calcium regulates vesicle replenishment at the cone ribbon synapse. J. Neurosci. 2010; 30:15866–15877. [PubMed: 21106825]
74. Hosoi N, et al. Quantitative analysis of calcium-dependent vesicle recruitment and its functional role at the calyx of Held synapse. J. Neurosci. 2007; 27:14286–14298. [PubMed: 18160636]
75. Stevens CF, Wesseling JF. Activity-dependent modulation of the rate at which synaptic vesicles become available to undergo exocytosis. Neuron. 1998; 21:415–424. [PubMed: 9728922]
76. Dittman JS, Regehr WG. Calcium dependence and recovery kinetics of presynaptic depression at the climbing fiber to Purkinje cell synapse. J. Neurosci. 1998; 18:6147–6162. [PubMed: 9698309]
77. Pan B, Zucker RS. A general model of synaptic transmission and short-term plasticity. Neuron. 2009; 62:539–554. [PubMed: 19477155]
78. Sakaba T, Neher E. Calmodulin mediates rapid recruitment of fast-releasing synaptic vesicles at a calyx-type synapse. Neuron. 2001; 32:1119–1131. [PubMed: 11754842]
79. Junge HJ, et al. Calmodulin and Munc13 form a Ca^{2+} sensor/ effector complex that controls short-term synaptic plasticity. Cell. 2004; 118:389–401. [PubMed: 15294163]
80. Wölfel M, et al. A mechanism intrinsic to the vesicle fusion machinery determines fast and slow transmitter release at a large CNS synapse. J. Neurosci. 2007; 27:3198–3210. [PubMed: 17376981]
81. Wadel K, et al. The coupling between synaptic vesicles and Ca^{2+} channels determines fast neurotransmitter release. Neuron. 2007; 53:563–575. [PubMed: 17296557]

82. Weyhersmüller A, et al. Rapid active zone remodeling during synaptic plasticity. J. Neurosci. 2011; 31:6041–6052. [PubMed: 21508229]
83. Verhage M, Sørensen JB. Vesicle docking in regulated exocytosis. Traffic. 2008; 9:1414–1424. [PubMed: 18445120]
84. Wang X, et al. A protein interaction node at the neurotransmitter release site: domains of Aczonin/Piccolo, Bassoon, CAST, and Rim converge on the N-Terminal domain of Munc13-1. J. Neurosci. 2009; 29:12584–12596. [PubMed: 19812333]
85. Deng L, et al. RIM proteins activate vesicle priming by reversing autoinhibitory homodimerization of Munc13. Neuron. 2011; 69:317–331. [PubMed: 21262469]
86. Kiyonaka S, et al. RIM1 confers sustained activity and neurotransmitter vesicle anchoring to presynaptic Ca^{2+} channels. Nat. Neurosci. 2007; 10:691–701. [PubMed: 17496890]
87. He L, et al. Compound vesicle fusion increases quantal size and potentiates synaptic transmission. Nature. 2009; 459:93–97. [PubMed: 19279571]
88. Walter AM, et al. Multiple Ca^{2+} sensors in secretion: teammates, competitors or autocrats? Trends Neurosci. 2011; 34:487–497. [PubMed: 21831459]
89. LoGiudice L, et al. Mobility and turnover of vesicles at the synaptic ribbon. J. Neurosci. 2008; 28:3150–3158. [PubMed: 18354018]
90. Zenisek D, et al. Transport, capture and exocytosis of single synaptic vesicles at active zones. Nature. 2000; 406:849–854. [PubMed: 10972279]
91. Mennerick S, Matthews G. Ultrafast exocytosis elicited by calcium current in synaptic terminals of retinal bipolar neurons. Neuron. 1996; 17:1241–1249. [PubMed: 8982170]
92. Lorteije JAM, et al. Reliability and precision of the mouse calyx of Held synapse. J. Neurosci. 2009; 29:13770–13784. [PubMed: 19889989]
93. Silver RA, et al. Locus of frequency-dependent depression identified with multiple-probability fluctuation analysis at rat climbing fibre-Purkinje cell synapses. J. Physiol. 1998; 510:881–902. [PubMed: 9660900]
94. Kawasaki F, Ordway RW. Molecular mechanisms determining conserved properties of short-term synaptic depression revealed in NSF and SNAP-25 conditional mutants. Proc. Natl. Acad. Sci. U.S.A. 2009; 106:14658–14663. [PubMed: 19706552]
95. Ruiz R, et al. Active zones and the readily releasable pool of synaptic vesicles at the neuromuscular junction of the mouse. J. Neurosci. 2011; 31:2000–2008. [PubMed: 21307238]
96. Markram H, et al. Differential signaling via the same axon of neocortical pyramidal neurons. Proc. Natl. Acad. Sci. U.S.A. 1998; 95:5323–5328. [PubMed: 9560274]
97. Gundelfinger ED, Fejtova A. Molecular organization and plasticity of the cytomatrix at the active zone. Curr. Opin. Neurobiol. 2011; 22:423–430. [PubMed: 22030346]
98. Waites CL, Garner CC. Presynaptic function in health and disease. Trends Neurosci. 2011; 34:326–337. [PubMed: 21596448]
99. Lupashin V, Sztul E. Golgi tethering factors. Biochim. Biophys. Acta. 2005; 1744:325–339. [PubMed: 15979505]
100. Schmitt HD, Jahn R. A tethering complex recruits SNAREs and grabs vesicles. Cell. 2009; 139:1053–1055. [PubMed: 20005800]
101. Fenster SD, et al. Piccolo, a presynaptic zinc finger protein structurally related to bassoon. Neuron. 2000; 25:203–214. [PubMed: 10707984]
102. Dani A, et al. Superresolution imaging of chemical synapses in the brain. Neuron. 2010; 68:843–856. [PubMed: 21144999]
103. Limbach C, et al. Molecular in situ topology of Aczonin/Piccolo and associated proteins at the mammalian neurotransmitter release site. Proc. Natl. Acad. Sci. U.S.A. 2011; 108:E392–E401. [PubMed: 21712437]
104. Altrock WD, et al. Functional inactivation of a fraction of excitatory synapses in mice deficient for the active zone protein bassoon. Neuron. 2003; 37:787–800. [PubMed: 12628169]
105. Kittel RJ, et al. Bruchpilot promotes active zone assembly, Ca^{2+} channel clustering, and vesicle release. Science. 2006; 312:1051–1054. [PubMed: 16614170]

106. Gracheva E, et al. Direct interactions between *C. elegans* RAB-3 and Rim provide a mechanism to target vesicles to the presynaptic density. Neurosci. Lett. 2008; 444:137–142. [PubMed: 18721860]

107. Kaeser PS. Pushing synaptic vesicles over the RIM. Cell. Logist. 2011; 1:106–110. [PubMed: 21922075]

108. Zanazzi G, Matthews G. The molecular architecture of ribbon presynaptic terminals. Mol. Neurobiol. 2009; 39:130–148. [PubMed: 19253034]

109. Toonen RF, et al. Dissecting docking and tethering of secretory vesicles at the target membrane. EMBO J. 2006; 25:3725–3737. [PubMed: 16902411]

110. Gracheva EO, et al. Differential regulation of synaptic vesicle tethering and docking by UNC-18 and TOM-1. Front. Synaptic Neurosci. 2010; 2:141. [PubMed: 21423527]

111. Gerber SH, et al. Conformational switch of Syntaxin-1 controls synaptic vesicle fusion. Science. 2008; 321:1507–1510. [PubMed: 18703708]

112. Denker A, Rizzoli SO. Synaptic vesicle pools: an update. Front. Synaptic Neurosci. 2010; 2:135. [PubMed: 21423521]

113. Shupliakov O, et al. How synapsin I may cluster synaptic vesicles. Semin. Cell Dev. Biol. 2011; 22:393–399. [PubMed: 21798362]

114. Gabriel T, et al. A new kinetic framework for synaptic vesicle trafficking tested in synapsin knock-outs. J. Neurosci. 2011; 31:11563–11577. [PubMed: 21832187]

115. Gaffield MA, Betz WJ. Synaptic vesicle mobility in mouse motor nerve terminals with and without Synapsin. J. Neurosci. 2007; 27:13691–13700. [PubMed: 18077680]

116. Lee JS, et al. Actin-dependent rapid recruitment of reluctant synaptic vesicles into a fast-releasing vesicle pool. Proc. Natl. Acad. Sci. U.S.A. 2012; 109:E765–E774. [PubMed: 22393020]

117. Srinivasan G, et al. The pool of fast releasing vesicles is augmented by myosin light chain kinase inhibition at the calyx of Held synapse. J. Neurophysiol. 2008; 99:1810–1824. [PubMed: 18256166]

118. Sankaranarayanan S, et al. Actin has a molecular scaffolding, not propulsive, role in presynaptic function. Nat. Neurosci. 2003; 6:127–135. [PubMed: 12536209]

119. Siksou L, et al. Three-dimensional architecture of presynaptic terminal cytomatrix. J. Neurosci. 2007; 27:6868–6877. [PubMed: 17596435]

120. Jiao W, et al. Two pools of vesicles associated with the presynaptic cytosolic projection in *Drosophila* neuromuscular junctions. J. Struct. Biol. 2010; 172:389–394. [PubMed: 20678577]

121. O'Rourke NA, et al. Deep molecular diversity of mammalian synapses: why it matters and how to measure it. Nat. Rev. Neurosci. 2012; 13:365–379. [PubMed: 22573027]

Europe PMC Funders Author Manuscripts

Europe PMC Funders Author Manuscripts

Box 1

Impact of the size of the release-ready pool (RRP) of vesicles on estimates of the reloading rate

To sustain a particular level of release, the required rate of vesicle reloading depends on the size of the RRP at a synaptic connection. RRP can be defined functionally: for central and NMJ synapses the RRP is the total number vesicles that could potentially be released by a single action potential at a synaptic connection, whereas at analog ribbon-type synapses (and for presynaptic capacitance measurements) the RRP is the number of vesicles released in the initial, rapid phase of release during a depolarizing pulse. To illustrate how the size of the RRP affects release, we compare the mean properties of two central synapses, one with a RRP size of 2 and a vesicular release probability (p_{rv}) of 0.6 (Figure Ia) and another with a RRP of 6 and a p_{rv} of 0.2 (Figure Ib). Both result initially in the release of on average 1.2 vesicles per action potential (quantal content of 1.2). Assuming a reloading rate-constant per release-ready vesicle (k) of 30 s^{-1} and 10 s^{-1}, respectively, the sustained release during 100 Hz transmission (10 APs) is in both cases approximately 0.4 vesicles per AP (neglecting any facilitating mechanisms; see equation 5 in [96]). Thus, despite the lower k, both scenarios result in the same amount of sustained release because, with a RRP of six vesicles, each vesicle is released less frequently and can afford slower reloading. The time-course of depression is slightly faster in the small RRP synapse. Experimental estimation of k therefore critically depends on the correct determination of the RRP size, at least when analyzing sustained release. By contrast, the recovery from synaptic depression is independent of the size of the RRP [i.e., the time-constant of recovery is the inverse of k; 33 ms (left) and 100 ms (right)]. However, the recovery from synaptic depression must be analyzed with caution because it is often influenced by other time-dependent factors such as presynaptic facilitation in p_{rv}, the recovery from Ca^{2+}-dependent modulation of the presynaptic Ca^{2+}-currents, and the recovery from postsynaptic depression.

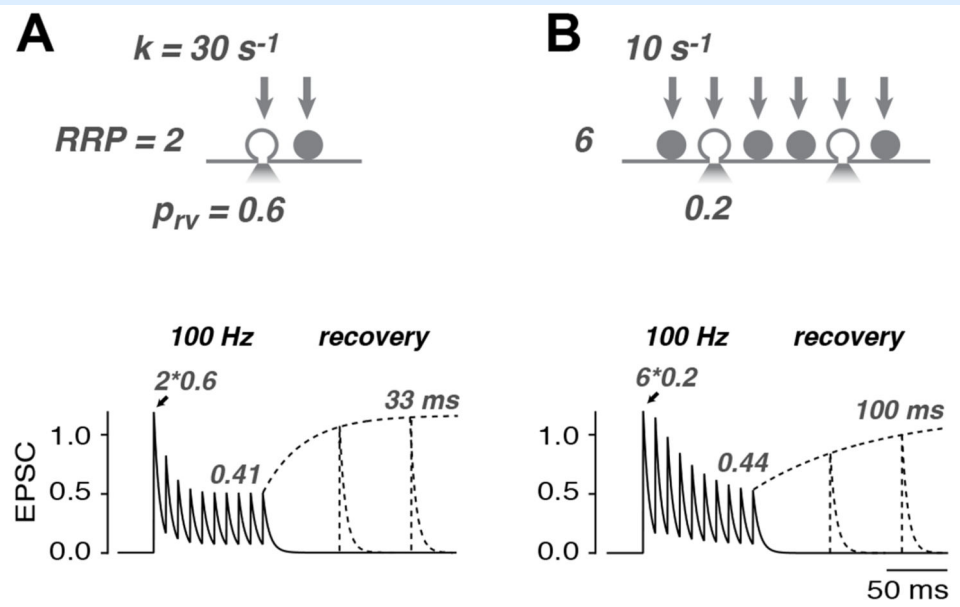

Figure I.

Properties of two central synapses with different RRP sizes. Top: illustration of a synapse with a small release-ready pool (RRP) and rapid vesicle reloading (a), and a larger RRP and slower vesicle reloading (b). Bottom: both synapses exhibit a similar sustained release rate as shown in this simulation. However, to achieve this a threefold faster reloading rate is required for the smaller RRP. The time-constant of recovery reveals the rate of vesicle reloading when there are no other time-dependent processes involved (see Box 1 in main text).

Box 2

Molecular nature of the vesicle tethers

Many proteins seem to be involved in building the vesicle-tethering cytomatrix at the AZ [18,97], and alterations of specific molecules have been linked to the etiology of several neurodevelopmental and neurodegenerative diseases [98]. Although there is some information on Golgi- and endoplasmic reticulum-resident vesicle-tethering factors [99,100], the molecular composition of the cytomatrix that tethers vesicles at the AZs of synapses is not well understood. Some of the possible vesicle-tethering proteins – excluding the SNARE complexes – are listed below:

- Piccolo and Bassoon [~4000 and ~5000 amino acids (aa), respectively] are highly homologous AZ proteins [101] and are orientated similarly within the AZ [102,103]. No obvious ultrastructural alterations were resolved in Bassoon mutants [104], but a reduction in the number of tethered vesicles within 150 nm of the membrane was observed in Bassoon/Piccolo double mutants [67].
- Bruchpilot (~1700 aa) is a *Drosophila* protein, has some homology to the vertebrate ELKS/CAST, is an integral component of the electron-dense structure [23], clusters Ca^{2+} channels [105], and its C-terminal 17-aa are required for vesicle tethering [27].
- Rim (~1600 aa) tethers vesicles and Ca^{2+} channels [68,69,106,107] and alterations in vesicle distribution and cytomatrix architecture might be resolvable in RIM1α knockout mice (Fernández-Busnadiego et al., Society for Neuroscience abstract 318.09, 2011).
- Ribeye (~900 aa) is the only known protein specific for synaptic ribbons [108], but the protein that tethers vesicles to the ribbon is currently not known.
- Munc18 (~600 aa) has been shown to interact with syntaxin to tether dense-core vesicles at the plasma membrane of chromaffin cells [109] and synaptic vesicles at the NMJ of *Caenorhabditis elegans* [110]. However, a normal density of docked vesicles was observed at vertebrate central AZs upon interference with binding of syntaxin to Munc18 [111].
- Synapsin (~600 aa) crosslinks vesicles and thus tethers vesicles indirectly at the AZ [112,113]. Interference with synapsin or synapsin phosphorylation alters vesicle-reloading kinetics [114], but see [115].
- An actin–myosin-mediated scaffold (actin ~400 and myosin ~2000 aa) may mediate the delivery of synaptic vesicles to the AZ [116–118].

Europe PMC Funders Author Manuscripts

Box 3

Outstanding questions

- Although the speed of vesicle reloading is likely to differ between synapses (e.g., [121]), it is currently unclear to what extent methodological differences contribute to the divergent estimates of the rate of vesicle reloading (see Table 1 in main text).
- Does the coupling distance between the fusion sensor and the Ca^{2+} channels increase during high-frequency transmission? This question has only been addressed at a limited number of synapse (e.g., [81]), but the answer might allow the mechanisms illustrated in Figure 3 in main text to be distinguished.
- What are the molecular identities of the tethers?
- What are the interaction partners of the tethers?
- What is the temporal sequence of vesicle binding to the tethers during vesicle docking and priming? In other words, do vesicles first bind to larger tethers and then sequentially to shorter ones, before finally reaching the membrane in a primed state?

Europe PMC Funders Author Manuscripts

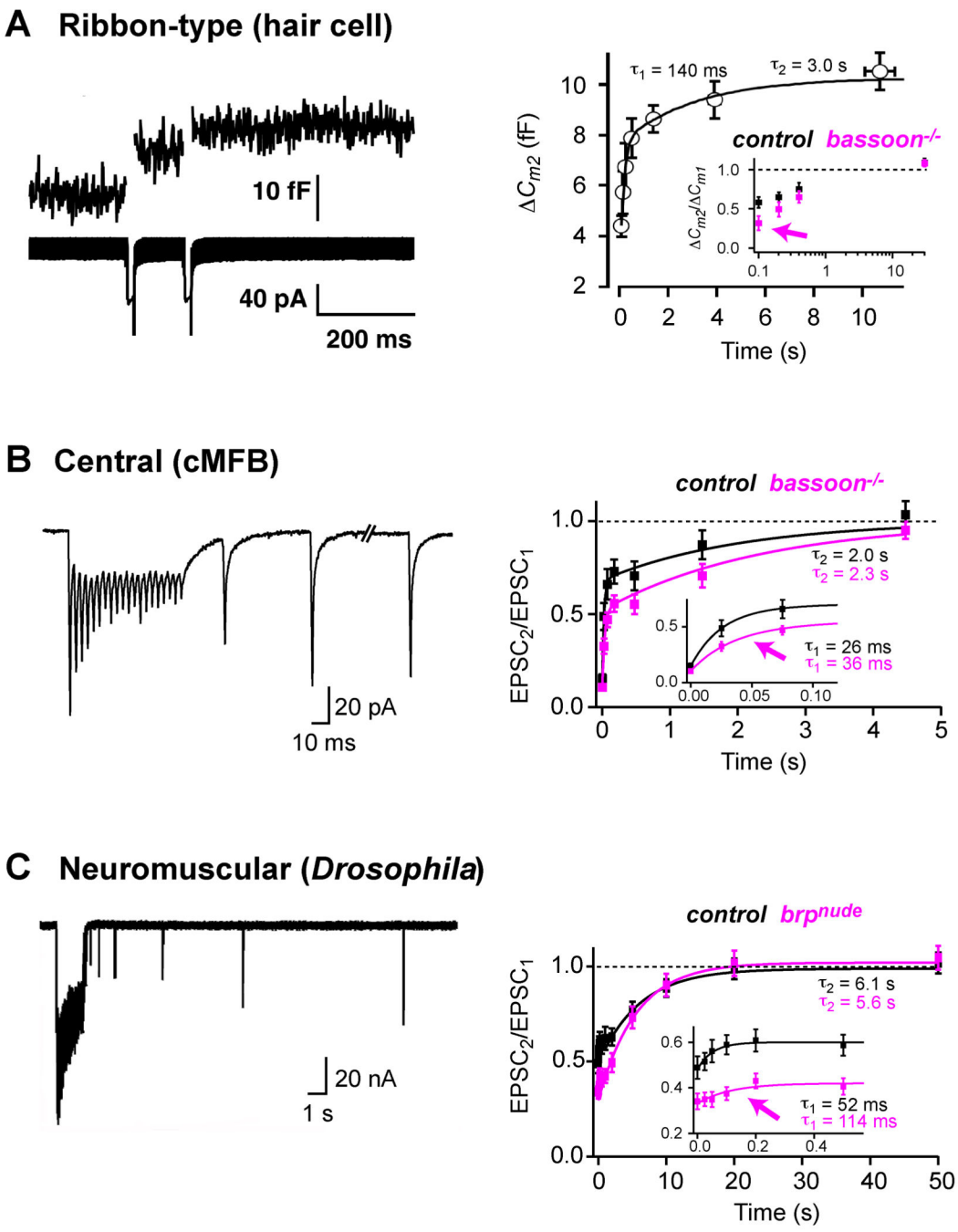

Figure 1.

Deletion or mutation of putative vesicle tethering proteins impairs the rapid component of recovery from synaptic depression. (a–c) Examples of a ribbon-type, central, and NMJ synapse with two kinetic components of recovery from synaptic depression (also see Table 1 in main text). Deletion of putative vesicle-tethering proteins or specific interference with vesicle tethering (magenta) resulted in all three examples in a slower recovery from synaptic depression [22,27,29]. The preferentially impaired first component of recovery (magenta arrows) suggests that vesicle tethering is important for activity-dependent speeding of

vesicle reloading. (**a**) Ribbon synapses. Left: presynaptic recordings from a hair cell ribbon synapse. Capacitance increases (upper trace) and Ca^{2+} current (lower trace) elicited by a paired-pulse paradigm (two 15 ms depolarizations). Right: average capacitance increases of the 2nd pulse of paired depolarizations (ΔC_{m2}) versus inter-pulse interval superimposed with a bi-exponential fit [71]. Inset: capacitance increases of the 2nd pulse of paired depolarizations (20 ms) normalized to the 1st response ($\Delta C_{m2}/\Delta C_{m1}$) versus inter-pulse interval for control (black) and Bassoon mutants (magenta) [22]. (**b**) Central synapses. Left: excitatory postsynaptic currents (EPSCs) recorded at a cerebellar mossy fiber to granule-cell synapse elicited by 300 Hz stimulation followed by test stimuli of increasing intervals. Right: average EPSC amplitude during recovery from depression normalized to the 1st EPSC amplitude for control (black) and Bassoon mutants (magenta) superimposed with bi-exponential fits [29]. Inset: the fast component of recovery on expanded scale. (**c**) Neuromuscular synapses. Left: EPSCs recorded at the NMJ of 3rd instar *Drosophila* larvae elicited by 60 Hz stimulation followed by test stimuli of increasing intervals. Right: average EPSC amplitude during recovery from depression normalized to the 1st EPSC amplitude for control (black) and Bruchpilot mutants lacking the last 17 C-terminal amino acids (brp^{nude}, magenta) superimposed with exponential fits to the slow component [27]. Inset: corresponding fits to the fast component. Adopted, with permission, from [71] and [22] (a), [29] (b), and [27] (c).

Europe PMC Funders Author Manuscripts

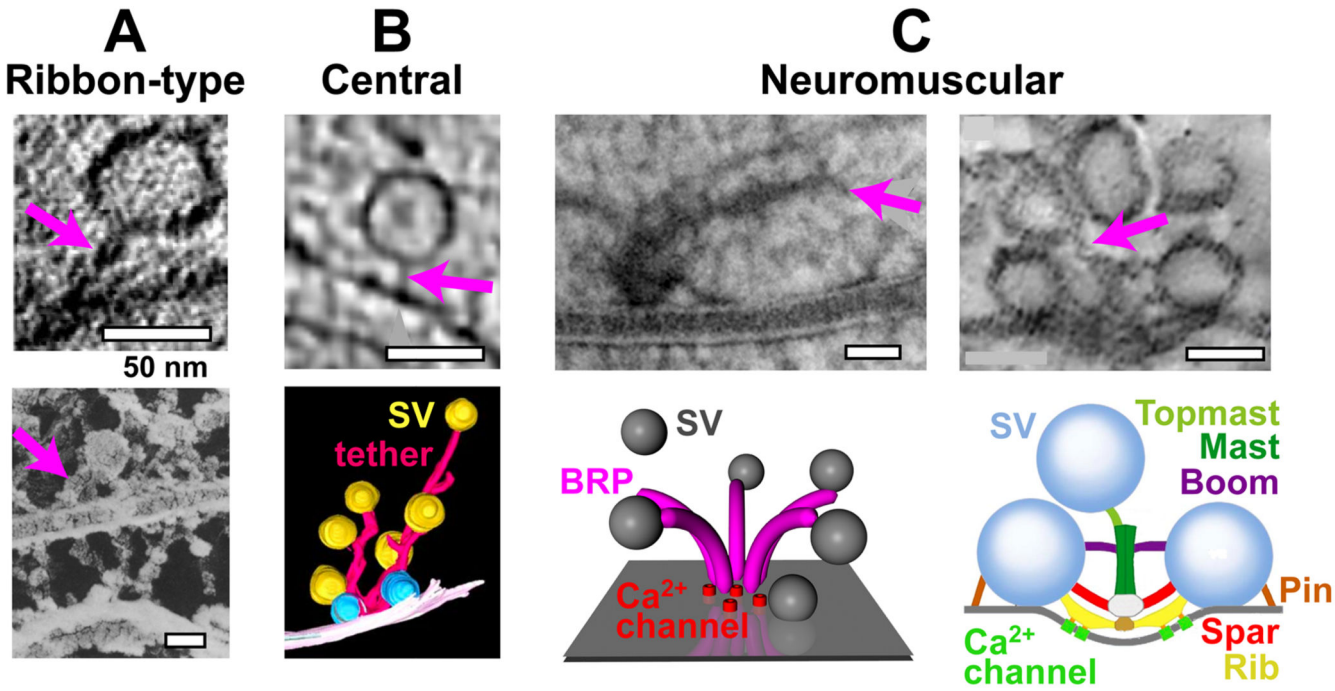

Figure 2.

Vesicle tethering at ribbon-type, central, and neuromuscular junction (NMJ) synapses. Examples of vesicle tethers (magenta arrows). (**a**) Ribbon synapses. Top: electron micrograph (EM) of a vesicle tethered at the plasma membrane of a ribbon-type mouse inner hair-cell synapse [22]. Bottom: EM of a cross-fractured synaptic ribbon (horizontal) with tethered vesicles [21]. (**b**) Central synapses. Top: electron tomographic slice of cerebrocortical synaptosomes [26]. Bottom: 3D reconstruction of vesicles and tethers [119]. (**c**) Neuromuscular synapses. Left: high-pressure freeze EM with filamentous structures at a *Drosophila* NMJ AZ (top) [23], consisting most likely of the *Drosophila* protein Bruchpilot (BRP), that has a funnel-like topology (bottom); SV, synaptic vesicle; adapted from [27], see also [120]. Right: electron tomographic slice of corresponding filamentous structures at the frog NMJ AZ (top), consisting most likely of different classes of AZ macromolecules, as illustrated in the schematic model (bottom) [25]. Adapted, with permission, from [22] and [21] (a), [26] and [119] (b), and [23], [27] and [25] (c).

Europe PMC Funders Author Manuscripts

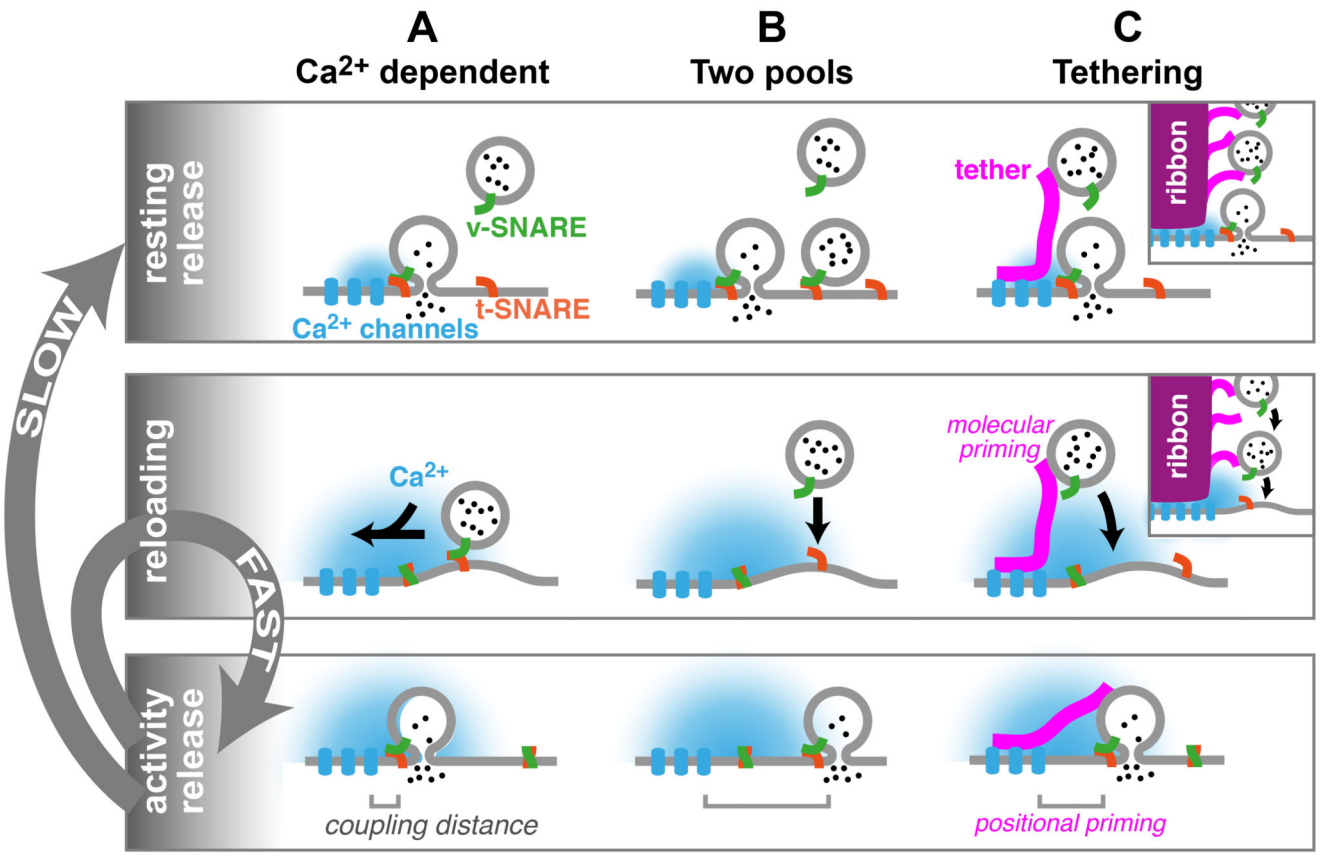

Figure 3.

Schematic illustrations of potential mechanisms underlying vesicle reloading and the putative role of tethers. Vesicular release under resting conditions (top) is followed by vesicle reloading mechanisms (middle) that allow repetitive release during synaptic activity (bottom). Although vesicle reloading during synaptic activity is fast, the complete recovery to the resting condition is slow (gray arrows). Three mechanisms explaining activity-dependent speeding of vesicle reloading are illustrated, although it is important to note that these mechanisms are not mutually exclusive. (**a**) Ca^{2+}-dependent model. Influx of Ca^{2+} through Ca^{2+} channels triggers the fusion of a vesicle which has undergone 'molecular' priming (illustrated by v- and t-SNARE assembly) and 'positional' priming (illustrated by the proximity of the fusion sensor to the Ca^{2+} channels, 'coupling distance') [31,32]. During activity, the Ca^{2+} concentration rises in the terminal, and reloading of vesicles to a molecular and positional primed state is accelerated [48,74]. After activity, Ca^{2+} decays and reloading slows. (**b**) Two-pools model. Two populations of vesicles with different release probabilities due to different coupling distances. After fusion of both docked vesicles, rapid molecular priming of vesicles is sufficient to sustain release of vesicles loosely coupled to Ca^{2+} channels during activity. The spatial and temporal extent of $[Ca^{2+}]$ may increase during sustained activity, augmenting this process. After activity, slower positional priming of a small subset of vesicles resupplies the pool of high release-probability vesicles [78]. (**c**) Tethering model. Vesicle tethers could accelerate vesicle reloading by (i) providing release-ready vesicles at AZs, (ii) constraining vesicles to dock closer to Ca^{2+} channels (positional

priming), and/or (iii) enriching priming factors on the vesicle (molecular priming). After activity, slow positional priming of vesicles closer to Ca^{2+} channels occurs as in panel (b). The inset illustrates vesicle tethering at ribbons, highlighting the similarities between vesicle tethering by ribbons at sensory synapses and by filamentous structures at central and neuromuscular junction (NMJ) synapses.

Europe PMC Funders Author Manuscripts

Table 1

Kinetics of recovery from synaptic depression and rate of vesicle reloading per release-ready vesicle at different types of synapses[a]

Synapse	Species	T (°C)	Recovery kinetics[b]		Reloading rate-constant[c]		Method	Refs
			τ_{fast} (s)	τ_{slow} (s)	max (1/s)	resting (1/s)		
Ribbon-type								
Bipolar cell	Goldfish	RT	0.640	31.0	(2)[d]	(0.03)	C_m	[72]
		RT	-[e]	-	4	-	TIRF	[90][f]
		RT	-	-	-	0.23	C_m	[91][g]
		RT	-	-	23	-	C_m	[15]
	Rat (P20)[h]	RT	0.400	5.9	8	(0.2)	Pair	[51]
Hair cell	Mouse	RT	0.140	3.0	50	(0.3)	C_m	[71][i]
		RT	-	-	70	-	C_m	[4]
	Bullfrog	RT	0.015	0.6	(67)	(1.7)	Pair	[5]
Central (Cerebellum and auditory only)								
Calyx of Held	Mouse (P13)	RT	0.052	1.1	(19)	(0.9)	Axon stim	[50]
	Mouse (P27)	36	0.050	2.0	(20)	(0.5)	Axon stim	[92]
	Rat (P9)	RT	-	-	3.3	0.1	C_m	[74]
	Rat (P14)	35	-	-	3.5	-	C_m	[34]
Cerebellar mossy fiber-granule cell	Mouse (P27)	37	0.026	2.0	70	0.5	Axon stim	[29]
	Rat (P27)	37	-	-	80	-	Axon stim	[9]
Cerebellar granule-stellate cell	Rat (P18)	35	-	-	63	-	Axon stim and α-LTX	[11]
Cerebellar parallel fiber-purkinje cell	Rat (P18)	34	-	-	30	2	Axon stim	[48]
	Rat (adult)	32	-	-	21	-	Axon stim	[12][j]
Cerebellar climbing fiber-purkinje cell	Rat (P13)	RT	0.300	2.7	(3)	(0.4)	Axon stim	[93]
	Rat (P13)	37	0.044	1.2	(23)	(0.8)	Axon stim	[76]
	Rat (P18)	34	-	-	20	0.7	Axon stim	[48]
Neuromuscular								
Muscle 6/7	*Drosophila* larvae	RT	0.052	6.1	(19)	(0.2)	*Axon stim*	[27]
		RT			15	0.05	*Axon stim*	[47]
Dorsal longitudinal flight muscle	*Drosophila* fly	33	0.040	1.5	(25)	(0.7)	*Axon stim*	[94]
Carpopodite extensor muscle (phasic junction)	Crayfish	RT	0.130	2.1	(8)	(0.5)	*Axon stim*	[77]
Levator auris longus muscle	Mouse (adult)	RT			2.3	1.1	*Axon stim*	[95][k]

[a] Abbreviations: axon stim, extracellular axonal stimulation; C_m, membrane capacitance measurements; α-LTX, a-latrotoxin; pair, pre- and postsynaptic whole-cell voltage-clamp recording; RT, room temperature; T, recording temperature; TIRF, total internal reflection fluorescence microscopy.

[b] Fast and slow time-constants (τ_{fast} and τ_{slow}, respectively) of recovery from synaptic depression.

[c] Rate-constant of vesicle reloading per release-ready vesicle both during (maximal rate) and after activity (resting rate).

[d] If the reloading rate-constants were not determined, the inverse of the time-constant of the recovery from depression is shown in brackets (see Box 1 in main text). However, this neglects any presynaptic changes in p_{rv} due to processes such as facilitation and postsynaptic contributions to the time-course of recovery from depression.

[e] -,Not determined.

[f] Mean latency of a newcomer vesicle was 250 ms during sustained depolarisations.

[g] Recovery from paired-pulse depression induced by 8 ms depolarizations with a time-constant of 4.3 s.

[h] P, postnatal day.

[i] Sustained exocytosis: 320 fF s^{-1}/(140 release-ready vesicles × 45 aF single-vesicle capacitance).

[j] Mean of estimates of the reloading time-constant of 30 and 65 ms.

[k] 40 quanta per action potential during 100 Hz (=4000 s^{-1})/1700 release-ready vesicles; 850 ms time-constant of recovery of the RRP.

Europe PMC Funders Author Manuscripts